Effect of sintering time on the photopthermal spectrum of the ceramic MnO_2-Y_2O_3-ZnO

Azmi Zakaria, Zahid Rizwan, Mansor Hashim, Abdul Halim Shaari, W. Mohmood Mat Yunus and Zainal Abidin Sulaiman
Department of Physics, Faculty of Science, Universiti Putra Malaysia, 43400 Serdang, Selangor, Malaysia

(Received 6 December 2006)

A powerful tool, photopyroelectric spectroscopy, for examining the optical properties as non-radiative de-excitation process for the ceramic (99.4-x) ZnO + 0.6 MnO_2 + x Y_2O_3, x = 0, 0.4, 0.8, 1.2, 1.6, mol%, is used. The ceramic was sintered at isothermal temperature 1275ºC for 1 and 5 hours to investigate its optical properties. The PPE spectroscopy is used to study the energy band-gap of the ceramic. The wavelength of incident light modulated at 9 Hz is kept in the range of 300 to 800 nm and the photopyroelectric spectrum with reference to the doping level is discussed. The band-gap energy (E_g) is estimated from the plot $(\rho h\upsilon)^2$ vs $h\upsilon$ and is decreased to 2.18, 2.14 eV at the at 0 mol% of Y_2O_3 for 1 and 5 hours sintering time, respectively. E_g is about constant at 2.190 ± .003, 2.160 ± .007 for 1 and 5 hours sintering time, respectively, for all doping level of Y_2O_3. The steepness factor σ_A (in A region) and σ_B (in B region) which characterizes the slop of exponential optical absorption is discussed with reference to the doping level of Y_2O_3. The X-ray diffractrometry shows that the crystal structure of the doped ceramic is rich with secondary phase Yttrium but very small few peaks of $ZnMnO_3$, Mn_3O_4 were found for the 5 hours sintering time. Microstructure and compositional analysis of the selected areas are analyzed using SEM and EDAX which shows the Yttrium-rich phase coexist in the grain boundaries and nodal points. The maximum relative density 93.6% is obtained for the ceramic for the 1 hour sintering time. The grain size decreases with the increase of Y_2O_3 mol% which shows that Y_2O_3 acts as a grain inhibitor.

I. INTRODUCTION

Zinc Oxide (ZnO), a white polycrystalline solid material and is n-type semiconductor material with a large energy band-gap 3.2 eV [1]. It crystallizes into a wurtzite structure, and is a complete hexagonal closed-packed (hcp) lattice with oxygen atoms inserted into the zinc hcp-lattice. It is widely used in the manufacturing of paints, rubber products, cosmetics, pharmaceuticals, floor covering, plastics, textiles, ointments, inks, soap, batteries, and also in electrical components such as piezoelectric transducers, phosphors, gas sensors and varistors [2,3].

The lattice constants of ZnO vary depending on how great is the unavoidable deviation from stochiometry towards an excess of the metal ($Zn_{1+x}O$). There are different opinions about the type of point defects that occur in the ZnO. The fact that the bonds in ZnO are 50-60% ionic [4] gives no indications to the type of defects. The measurements of the electron density [5] have shown that dominant defects are interstitial zinc ions and it was confirmed by Hagemark *et al.* [6] and Li *et al.* [7]. Other investigators, however, suggest oxygen vacancies, V_0 that predominates and this hypothesis never been refuted. The measurement of the content of excess zinc in $Zn_{1+x}O$ has indicated that the value of x ranges from 0 to 0.7 depending on the temperature and oxygen partial pressure [8].

Varistors are extensively used as protective devices to regulate transient voltage surges of unwanted magnitudes [9]. The exact role of many additives in the electronic structure of ZnO varistors is uncertain. ZnO based varistor is formed with other metal oxides of small amounts such as Bi_2O_3, Co_3O_4, Cr_2O_3 MnO, Sb_2O_3, etc. These additives are the main tools that are used to improve the non-linear response and the stability of ZnO varistor [10]. Varistor effect (highly nonohmic behavior in the *I-V* characteristics), which can be explained by the mechanism involving grain boundaries and the associated defect concentration gradients [11]. The distribution of vacancies and impurities as well as their behavior during annealing treatments appear as one of the factors that determine the electrical properties of ceramic ZnO. Much work has been done in *I-V* studies on ZnO based varistor by previous workers [10,12]. It is necessary to get information of optical absorption of ceramic ZnO doped with different metal oxides for the investigation of the electronic states of doped ceramic ZnO during sintering process and in this paper we discuss the photopyroelectric (PPE) spectroscopy of the Y_2O_3 doped ceramics MnO_2-ZnO.

II. MATERIALS AND METHODS

ZnO (99.9% purity) was doped with MnO_2 (99.999% purity) and Y_2O_3 (99.9% purity) according to the scheme (99.4-x) ZnO + 0.6 MnO_2 + xY_2O_3, x = 0, 0.4, 0.8, 1.2, 1.6 mol%. The 24 hours ball milled powder of each mole percent was pre-sintered at temperatures 750ºC for 2 hours. Then each sample was ground and polyvinyl alcohol (1.4 wt%) was mixed as a binder. The dried powder was pressed under a force of 800 kg cm^{-1} to form a disk of 10 mm diameter with 1 mm thickness. Finally the pellets were sintered at 1275ºC for 1 and 5 hour in air at the heating and cooling rate of 3ºC min^{-1}. The density was measured by geometrical method [13] using the average of 10 disks for each sample. The mirror like polished samples was thermally etched for the microstructure analysis using SEM. The average grain size was determined by the grain boundary-crossing method. The disks of each sample were ground to make a fine powder for the PPE spectroscopy and XRD analysis. Cu K_α radiation with PANAalytical (Philips) X'Pert Pro PW1830 was used for X-ray diffraction, and the XRD data were analyzed by using X'Pert High Score software for the identification of the crystalline phases.

PPE spectroscopy a powerful technique from photothermal science and is a non-radiative tool [14] to study optical properties of the materials. The method is based on photothermal effect where the PPE film transducer is used to detect the temperature variation from the light-induced periodic heating in the sample. When there is absorption of incident light, the non-radiative de-excitation processes with in the solid will cause the sample temperature to fluctuate, through heat diffusion to the surrounding PPE film. Due to this temperature change, a PPE voltage is observed in the PPE film. The measurement of PPE signal amplitude using the PPE spectrometer system to produce a PPE spectrum has been described elsewhere [15]. In the system, a light beam from 1 kW Xenon arc lamp (Oriel 6921) was mechanically chopped at 9 Hz. The scanning wavelengths range from 300 to 800 nm with a 2 nm step size.

Prior the PPE measurement, the fine powder sample was ground in deionised water and then a few drops of each mixture were dropped on the 1.5 cm^2 aluminium foil and dried in air to form a thin sample layer on the foil. The foil was placed in contact to polyvinylidene difluoride PPE film sensor [16] using a very thin layer of silver conductive grease. The true sample spectrum was obtained by normalisation with carbon black PPE spectrum. In determining the energy band-gap (E_g), it was assumed that the fundamental absorption edge of doped ZnO is due to the direct allowed transition. The optical absorption coefficient β varies with the excitation light energy $h\upsilon$ [17] and is given by the expression, $(\beta h\upsilon)^2 = C(h\upsilon - E_g)$ near the band gap, where $h\upsilon$ is the photon energy, C is the constant independent of photon energy, and E_g is the direct allowed energy band-gap. The PPE signal intensity ρ is directly proportional to β, hence $(\rho h\upsilon)^2$ is related to $h\upsilon$ linearly. From the plot of $(\rho h\upsilon)^2$ versus $h\upsilon$, the value of E_g is obtained by extrapolating the linear fitted region that crosses photon energy axis.

III. RESULTS AND DISCUSSION

XRD results (Fig. 1) show that all the samples have two major components, ZnO grains and intergranular layers composed of Y_2O_3 for the both sintering times 1 and 5 hours. But two very small peaks at an angle of 43.728º (ref. code 00-019-1461), 51.004º (ref. code 00-016-0154) of secondary phases $ZnMnO_3$, Mn_3O_4, respectively for 5 hours of sintering time at the 0 mol% of Y_2O_3.

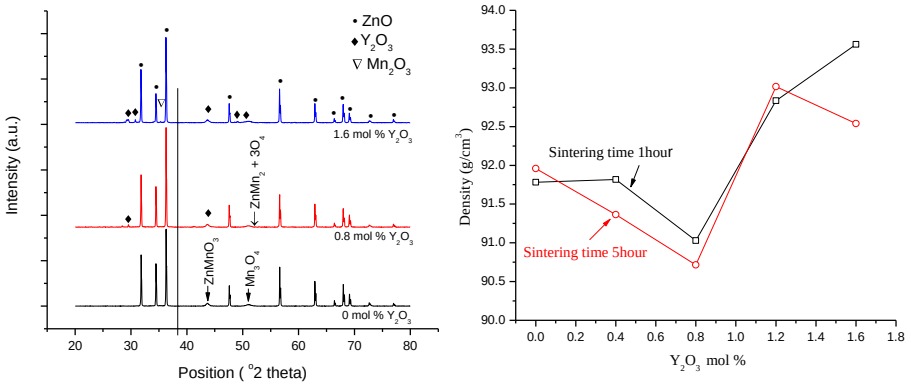

FIG. 1. XRD pattern for 5 hours sintering time (left) and the variation of density with the mol% of Y_2O_3 for 1 and 5 hours sintering time (right).

Few small peaks of Mn_2O_3 at 35.329º (ref. code 00-033-0900) and $ZnMn_2 + 3O_4$ at 50.978 (ref. code 00-007-0354) are present in the pattern. Peaks of Y_2O_3 (ref. code 01-074-0553) at angles of 29.517º, 30.805º, 43.787º, 49.114º are very clear.

The relative density of the ceramic ZnO doped at 0 mol% of Y_2O_3 is about 91.9% of the theoretical density (5.68 g/cm^3) and is decreased up to 0.8 mol% of Y_2O_3 doping level but this decrease is very small with the variation of 2%. This indicates the increase of pores in the ceramic. The density again increase with the increase of Y_2O_3 mol% as shown in Fig. 1 but this increase is about 4%. It is very clear that the density is not much changed with the increase of sintering time from 1 hour to 5 hour. This indicates that the pores are decreased at the higher doping level.

The grain size is 10 µm at 0 mol% of Y_2O_3 and is reduced to 4.3 µm with the increase of Y_2O_3 for 1 hour sintering time (Fig. 2). The grain size is 23.2 µm at 0 mol% of Y_2O_3 and is reduced to 7 µm with the increase of Y_2O_3 for 5 hours of sintering time. This indicates that the Y_2O_3 acts as a grain inhibitor. The decrease in the grain size from 20.06 µm to 10.9 µm is very clear with the decrease of sintering time 5 to 1 hour but this decrease is very slow at the higher doping level of Y_2O_3.

White clusters of Y_2O_3 are very clear and are verified by the EDAX analysis in the SEM micrograph (Fig. 3). Y_2O_3 is segregated at the grain boundaries and nodal points. Very small peak in the EDAX analysis was found at the surface of grains, indicating the possibility of interstitials of Y_2O_3.

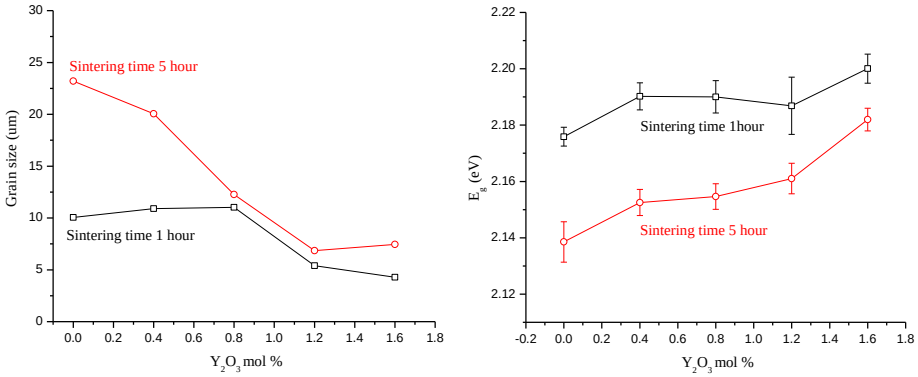

FIG. 2. Grain size (left) and Energy band gap dependence on the doping level of Y_2O_3 for 1 and 5 hours sintering time.

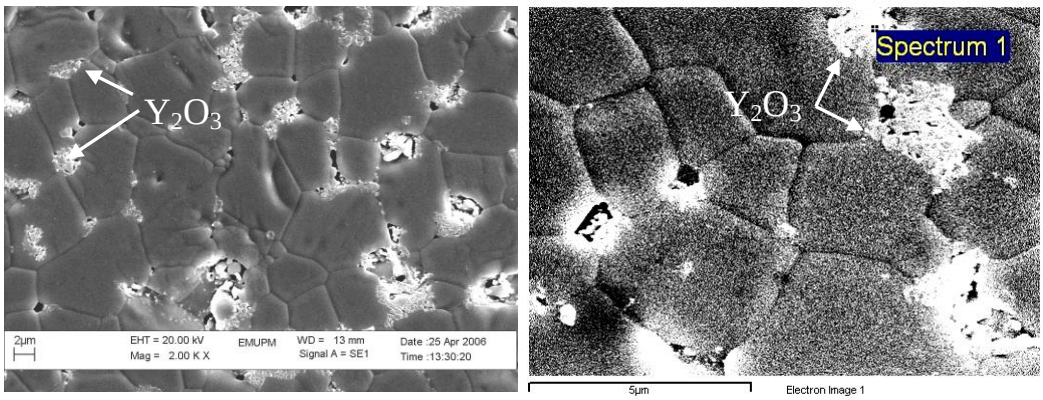

FIG. 3. SEM micrograph showing elemental distribution at different areas for 5 h at 1.6 mol%.

The E_g of the ceramic is 2.18, 2.14 eV at 0 mol% of Y_2O_3 for 1 and 5 hours sintering time, respectively Fig. 2. It is expected that this decrease in E_g, is due to the growth of interface states by Mn^{+2} ions. The decrease in the value of E_g is observed with the increase of the sintering time from 1 to 5 hours at all doping levels of Y_2O_3. The value of E_g is about constant at 2.19 eV for all mol% of Y_2O_3 but the value of E_g further increases to 2.20 eV at 1.6 mol% of Y_2O_3 for the sintering time of 1 hour. This may be due to the segregation of Y_2O_3 at the grain boundaries and nodal points. So the defects may reduce the interface states. The value of E_g is about constant at 2.15 eV at all doping levels of Y_2O_3 but it further increases to 2.18 eV at 1.6 mol% of Y_2O_3 for the sintering time of 5 hour. This may be due to the segregation of Y_2O_3 at the grain boundaries and nodal points. So the defects may reduce the interface states with the increase of Y_2O_3.

The steepness factor σ_A (in A-region), (Fig. 4), which characterizes the slop of exponential optical absorption decreases with the increase of mol% of Y_2O_3 indicating the decrease in the structural ordering for 1 hour sintering time. It is also decreased with the increase of sintering time indicating the structural disordering at the grain boundaries. The increase in E_g is also due to the structural disordering at the grain boundaries. The structural disordering is less obvious for the 1 hour sintering time. The steepness factor σ_B (in B-region) decreases with the increase of Y_2O_3 indicating the possibility of the increase of the defects for 1 hour sintering time. The decrease in σ_B with the increase of Y_2O_3 indicating the possibility of the increase in defect states for 5 hour sintering time. It is expected that the defect states are reduced at higher doping level of Y_2O_3. This decrease in the defect states may be due to MnO_2.

IV. CONCLUSION

XRD analysis shows the secondary phases ZnO and few peaks of $ZnMnO_3$, Mn_3O_4, for 5 hours of sintering time at the 0 mol% of Y_2O_3 and also few peaks of Mn_2O_3 and $ZnMn_2 + 3O_4$ are present at higher doping level of Y_2O_3. EDAX analysis shows the Y_2O_3 is segregated at the grain boundaries and nodal points. The maximum decrease in the density is at 0.8 mol% of Y_2O_3. Grain size decreases with the increase of Y_2O_3 for both sintering temperatures. E_g doped ceramic are 2.18, 2.14 eV at the 0 mol% of Y_2O_3 and is increased to a maximum value 2.20, 2.18 eV with the increase of Y_2O_3 for 1 and 5 hours sintering time, respectively. Doping level of Y_2O_3 produces the structural disordering.

ACKNOWLEDGEMENTS

The authors would like to thank the Ministry of Science, Technology and Innovation of Malaysia (MOSTI) for the financial support of this work under IRPA Grant No. 02-02-04-0132-EA001.

REFERENCES

[1] T. K. Gupta, "Application of zinc oxide varistors", J. Am. Ceram. Soc., **73(7)**, 1817-40 (1990).

[2] H. M. Lin, S. J. Tzeng, P. J. Hsiau and W. L. Tsai, "Electrode effects on gas sensing properties of nanocrystalline zinc oxide**",** Nanostruct. Mater., **12**, 465-77 (1998).

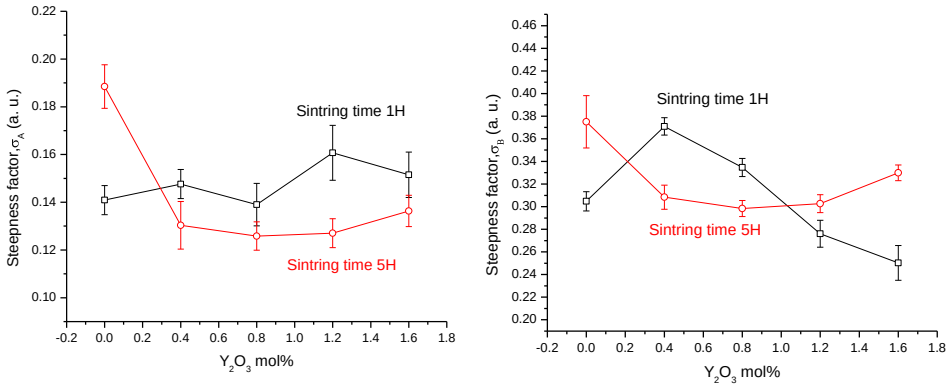

FIG. 4. Dependence of the steepness factor σ_A (left), σ_B (right) on Y_2O_3 mol%.

[3] D. C. Look, "Recent advances in ZnO materials and devices", Materials Science and Engineering, **B80**, 383-387 (2001).
[4] G. Neumann, *Non-stoichiometry and Defect Structure*, E. Kaldis (ed.), Currents Topics in Material Science, Vol. **7** (Zinc Oxide), North Holland, Amsterdam (1981), 153.
[5] G. P. Mohanty and L. V. Azaroff, "Electron density distribution in ZnO crystals", J. Chem. Phys., **35(4)**, 1268 (1961).
[6] K. I. Hagemark and L. C. Chacka, "Electrical transport properties of Zn doped ZnO", J. Solid State Chem., **15(3)**, 261 (1975).
[7] P. W. Li and K. I. Hagemark, "Low temperature electrical properties of Zn doped ZnO", J. Solid State Chem., **12(3/4)**, 371 (1975).
[8] Jae Shi Choi and Chul Hyun Yo, "Study of the nonstoichiometric composition of zinc oxide", J. Phys. Chem. Solids, **37(12)**, 1149 (1976).
[9] David R. Clarke, "Varistor ceramics", J. Am. Ceram. Soc., **8**, 485-501 (1999).
[10] K. Eda, "Zinc oxide varistors",. IEEE Elect. Insul. Mag., **5**, 28-41 (1989).
[11] R. Einzinger, "Grain junction properties of ZnO varistors", Appl. Surf. Sci., **3**, 390-408 (1979).
[12] Choon-Woo Nahm, "Electrical properties and stability of praseodymium oxide based ZnO varistor ceramics doped with Er_2O_3", J. Eu. Ceram. Soc., **23**, 1345-53 (2003).
[13] J. F. Wang, Wen-Bin Su, Hong-Cun Chen, Wen-Xin Wang and Guo-Zhong Zang, "(Pr, Co, Nb)-doped SnO_2 varistor ceramics", J. Am. Ceram. Soc., **88(2)**, 331-34 (2005).
[14] A. Minamide, M. Shimaguchi and Y. Tokunaga, "Study on photopyroelectric signal of optically opaque material measured by PVD film sensor", Jpn. J. Appl. Phys., **37**, 3144-47 (1998).
[15] A. Mandelis, "Frequency-domain photopyroelectric spectroscopy of condensed phases (PPES): A new, simple and powerful spectroscopic technique", Chem. Phys. Lett., **108**, 388-92 (1984).
[16] A. C. Tam and H. Coufal, "Photoacoustic generation and detection of 10-ns acoustic pulses in solids", Appl. Phys. Lett., **42**, 33-5 (1983).
[17] T. Toyoda, H. Nakanishi, S. Endo and T. Irie, "Fundamental absorption edge in semiconductor $CdInGaS_4$ at high temperatures", J. Phys. D Appl. Phys., **18**, 747-51 (1985).